Online at: https://researchtrendsjournal.com **ISSN No:** 2584-282X

INTERNATIONAL JOURNAL OF TRENDS IN EMERGING RESEARCH AND DEVELOPMENT

Volume 2; Issue 3; 2024; Page No. 203-209

Received: 04-02-2024
Accepted: 13-04-2024

A study on Asteroseismic determination of envelope helium abundance of sun-like stars

[1]Chandan Kumar and [2]Dr. Shailesh Kumar Singh

[1]Research Scholar, Department of Physics, Maharaja Agrasen Himalayan Garhwal University, Uttarakhand, India
[2]Professor, Department of Physics, Maharaja Agrasen Himalayan Garhwal University, Uttarakhand, India

Corresponding Author: Chandan Kumar

Abstract

A sun-like star has a number of areas where sound speed or its derivatives fluctuate quickly, such as the ionization zones of plentiful elements and the interfaces between radiative and convective regions. The discontinuity in the second derivative of the sound speed causes the sharp variations at the radiative and convective zone interfaces, while the local depression of the first adiabatic index, $\Gamma 1 = \partial \ln P$, where P and ρ stand for pressure and density, respectively, causes the sharp variations in the ionization zones. In the observed frequency range, the convective core boundary signature usually becomes aliased to very close to the surface and is indistinguishable from the background smooth component. We conducted systematic research to explore and remove any potential systematic uncertainty in the glitch analysis utilizing only the stellar models and the data for the real stars (the Sun and 16 Cyg A) along with their representative models. The Helium abundance is frequently considered as one of the free parameters that are changed to get the best fit to the data when more information is available, such as stellar oscillation frequencies and other spectroscopically determined stellar observables. Although these techniques provide more accurate constraints on the initial helium abundance, our incapacity to accurately simulate a star's surface may introduce systematic mistakes. The dynamical consequences of convection are not included in normal 1D models, which only handle convection in rough approximations. This results in significant variations in the near-surface layer structure, which causes a frequency-dependent inaccuracy in the frequencies known as the surface effect. The calculated stellar characteristics may have systematic inaccuracies if the surface term is eliminated.

Keywords: Asteroseismic, Envelope Helium Abundance, Sun Like Stars etc.

Introduction

The structure and evolution of normal stars are significantly influenced by helium, the second most abundant element in these stars. Unfortunately, due to their low surface temperatures, low-mass stars cannot have their helium abundance measured spectroscopically. As a result, a presumption regarding galactic chemical evolution determines the initial helium abundance of star models. For example, Yi = 0.23 + 2Zi is assumed in the construction of the Yale-Yonsei Isochrones (Demarque *et al*. 2004) [1]. The Padova tracks of Marigo *et al*. (2008) [2] assume Yi = 0.23+2.23Zi, but the Dartmouth tracks (Dotter *et al*. 2008) [3] assume Yi = 0.245 + 1.54Zi. For single stars calculated using such sets of isochrones and tracks, such ad hoc prescriptions might easily result in significant mistakes in the results.

Using the oscillation frequencies of a star, one can determine its helium abundance in a comparatively more straightforward manner. For instance, the quantity of Helium in the solar convection zone has been successfully ascertained by using the signal that Helium ionization leaves on the sound-speed profile (e.g., Basu & Antia 1995 [4], and references therein). The exact determination of the frequencies of around a few thousand modes with degrees ranging from 0 to 250 makes it easier to estimate the helium abundance Helio seismically for the Sun. In contrast, only modes of l = 0, 1, 2, and occasionally 3 can be identified for other stars. Therefore, a different method must be used to estimate the helium abundance. It may be possible to estimate the envelope Helium abundance of sun-like stars using the signal of the Helium glitch. The abundance of Helium determines the amplitude of the Helium signature;

the greater the abundance, the greater the amplitude. However, as demonstrated in Chapter 5, the amplitude of the Helium signature also depends on the mass and the effective temperature, thus selecting calibrating models that are sufficiently near is crucial. The potential use of this signature to ascertain the envelope Helium abundance of stars has been theoretically investigated. But as of yet, no star other than the Sun has had its helium content ascertained using this characteristic.

In this research, we use oscillation frequencies derived from 2.5 years of Kepler satellite data to calculate the envelope Helium abundance of 16 Cyg A & B (HD 186408 and 186427; KIC 12069424 and 12069449). These stars are some of the brightest in the Kepler area of view and constitute a binary system. In order to constrain the parameters of the stars, a three-month time series was analyzed. The results indicated that the stars are slightly older and more massive than the Sun. The stars were 6.8 ± 0.4 Gyr old, with initial helium abundance and metallicity of Yi = 0.25 ± 0.01 and Zi = 0.024 ± 0.002, respectively, who used the oscillation frequencies and spectroscopic constraints on the effective temperature and metallicity of the stars. The masses of the A and B components are 1.11 ± 0.02 M and 1.07 ± 0.02 M⊙, respectively, according to their estimations. Somewhat higher helium abundances for these stars using a similar methodology. The helium abundance numbers derived from the aforementioned techniques typically rely on the stellar models' input physics and the way surface effects are adjusted. Therefore, it is necessary to determine the present Helium abundance in the envelope in a more direct manner.

Research Methodology

Methods used to estimate the amplitude of Helium signature

To ascertain the envelope Helium abundance of 16 Cyg A & B, we employ three distinct methods to match the glitch signatures and two distinct measurements of the amplitude of the Helium signature. In each of these approaches, we calculate the calibration's amplitude averaged across the frequency range employed in the fit. Below is a brief description of the third way.

Fitting frequencies directly

This is another well-known technique for extracting the glitch signature. Although I haven't performed the calculations using this method (which was done by Faria and Monteiro), some results are displayed for comparison. With the exception of how the smooth component is handled and how the oscillatory function is expressed, this approach is comparable to Method A. The method here is to fit the signatures of the glitches after first fitting a smooth function of radial order to all the modes of the same degree and removing the smooth component. This technique calibrates using the amplitude of the helium signature at a reference frequency.

Calibration models

We must compare the measured amplitudes of the Helium signature to those computed for stellar models with varying Helium abundances in order to ascertain the Helium abundance of the stars. Three sets of models were used: one with YREC and two built with MESA for two distinct metallicity mixtures. Each set's models were built according to distinct principles, and the models used for calibration were chosen based on distinct standards. Below is a description of the models and the selecting procedure.

MESA models

With the exception of the overshoot, the models are produced using the input physics. In order to convert the observed [Fe/H] to Z required for the models, we build models assuming two distinct values of the solar metallicity. Keep in mind that the true value of the solar metallicity is still unknown. For many years, GS98's solar abundances with Z/X = 0.023 were widely utilized, and solar models built using these abundances met helioseismic constraints fairly well.

Results and Discussion

The solar abundance of heavy elements, was significantly lower, with Z/X = 0.0165, after they recalculated the solar abundances using a 3D model atmosphere and NLTE corrections for several lines. Additionally, the relative abundances of several elements were altered. The abundances were further updated to Z/X = 0.018. We have yet to address the difference between the lower abundances and helio-seismic constraints. In this work, we employed both the GS98 and AGSS09 combinations of heavy elements to evaluate the impact of this uncertainty on the final calculation of Helium abundance. Z for the models was derived for a given [Fe/H] assuming that [Fe/H] = 0 corresponds to Z/X = 0.023 for the GS98 mixture and Z/X = 0.018 for the AGSS09 mixture. Opacities were computed considering the various heavy-element mixes.

For 16 Cyg A & B, we built models with two distinct metallicity mixtures on a uniform grid of stellar characteristics. M ∈ 0.91 − 1.17M⊙, Yi ∈ 0.22 − 0.35, [Fe/H] i ∈ 0.12 − 0.26 dex, and αMLT ∈ 1.9 − 2.3 were the range of values in the grid. The corresponding step sizes were 0.02 M⊙, 0.02 dex, 0.02, and 0.05. Only when the evolutionary track enters a 4D box made up of the 2σ uncertainties in the measured Teff, L, [Fe/H], as shown in Table-1, was a model with a specific M, Yi, Zi, and αMLT chosen as an acceptable model of the star. For all components, the surface metallicity reported by Ramírez *et al.* (2009) [5] is not exactly the same, measuring 0.096 ± 0.026 dex for 16 Cyg A and 0.052 ± 0.021 dex for 16 Cyg B. Nonetheless, we assume that the two stars' metallicities are equal, 0.096 ± 0.040 dex, with a higher degree of uncertainty because they are fairly comparable. This may be supported by the fact that the stars should have the identical starting metallicities because they constitute a binary system. By reducing the discrepancy between the observed and surface corrected model frequencies, more degeneracy in the 4D box is removed. Thus, for 16 Cyg A and 16 Cyg B, we obtain two model ensembles each, which match to the two abundance choices of GS98 and AGSS09. However, they are not the last calibration model sets. The age of the models in each of these ensembles varies by around 5 Gyr. We employ an additional selection process that is explained below, which accounts for the requirement that 16 Cyg A and 16 Cyg B be of the same age. In order to quantify the impact of the uncertainty in the solar metallicity on our

results, models built using the AGSS09 mixture are treated differently from those built using the GS98 mixture.

Table 1: Various observables used to constrain the models of 16 Cyg A and B. Surface metallicity was assumed to be same for both components with increased uncertainty. Average large and small separations were calculated using observed frequencies

Observable	16 Cyg A	16 Cyg B	Reference
$T_{\rm eff}$	5839±42 K	5809±39 K	White et al. (2013)
log g	4.29±0.02 dex	4.36±0.02 dex	White et al. (2013)
L	1.56±0.05 $L_{\odot}$	1.27±0.04 $L_{\odot}$	Metcalfe et al. (2012)
[Fe/H]	0.096±0.040 dex	0.096±0.040 dex	Ramírez et al. (2009)
$\langle\Delta\nu\rangle_0$	102.9±0.2 μHz	116.5±0.2 μHz	...
$\langle\delta\nu_{0,2}\rangle$	5.82±0.03 μHz	6.70±0.03 μHz	...

To verify that the two components of the binary do, in fact, have identical ages, we first ascertain their individual ages once more using the procedure outlined. The standard χ2 for 16 Cyg A & B has terms that correspond to Teff, L, log g, [Fe/H], ▨Δν⟩0, and ⟨δν0,2⟩. It should be mentioned that the interferometric radii are found to be compatible with the final model radii for both stars, even if the radii of the two components have been determined with interferometry. Nevertheless, we do not utilize the radii to constrain the ages. A linear fit to the 12 radial mode oscillation frequencies as a function of n is used to determine ▨Δν⟩0. The ▨δν0,2⟩ is computed using the same 12 radial modes and matching quadrupole modes. The average big and small separations between the models and the observation are computed using the same set of modes. The surface effect causes systematic uncertainty in the model frequencies. We notice that ▨Δν⟩0 is consistently greater than the observed value by roughly 1μHz for our acceptable models. The differential form of the Duvall Law, is used to estimate the precise shift. This form breaks down the frequency differences between a model and observation into two components: one that is primarily the surface term and the other that depends on the interior structural differences. Before being compared to the observed values of 16 Cyg A & B, the models' ▨Δν⟩0 values are adjusted for the surface term. The approximate envelope of the standard χ2 comprising the aforementioned terms is displayed as a function of the reference age. For a certain assumed metallicity mixture, it is evident that the curves have a well-defined minimum that provides the best model and the best estimate of the age of each individual star. When using the GS98 mixture, the ages for 16 Cyg A and B are 6.9 ± 0.4 Gyr and 6.6 ± 0.4 Gyr, respectively. The ages are 7.1 ± 0.4 Gyr and 6.7 ± 0.4 Gyr for the AGSS09 combination, respectively. The two stars' ages are thus determined to be quite near to one another, and the values agree with those.

Using the procedure outlined, we ascertain the binary system's common age. As a function of the reference age, the approximate envelope of the standard χ2 with terms corresponding to both components is displayed. Once more, the resulting curves have a clearly defined minimum that provides the best estimates of the stars' common age and the best models. According to estimates, the binary system is 6.9 ± 0.3 Gyr old for the AGSS09 mixture and 6.7 ± 0.3 Gyr old for the GS98 mixture. Therefore, we discover that the age is not greatly impacted by the mixing of heavy metals. Houdek & Gough (2011) [6] have pointed out that in addition to δν0,2, we can use coefficients of a higher order asymptotic formula for oscillation frequency to determine the age more precisely, as these are more sensitive to the sound speed variation in the stellar core. This means that the age difference between models of two mixtures may become significant when the stellar parameters and the oscillation frequencies are known more precisely. Whether these phrases can be more precisely identified from the currently observed frequencies is unclear, though.

Models having ages within 1σ of the previously established common ages are removed from the ensembles. We are left with over 450 models at the end of this selection process, including almost 100 models for a star with a specific metallicity combination and a range of mass, chemical composition, mixing-length, and age. We have two sets of calibrating models for each component of the two metallicity mixtures, GS98 and AGSS09.

YREC models: The models from YREC are also utilized for calibration in addition to the models already mentioned. Although Basu completed the modelling using YREC, I did not; however, some findings are displayed for comparison.

Fit to the oscillation frequencies of 16 Cyg A & B

We use the observed frequencies calculated using the method outlined using 2.5 years of Kepler simple-aperture-photometry light curves that have been high-pass filtered with a 4-day triangular smooth and corrected. Table-2 lists the observed frequencies used in this work. Except for the final two modes for 16 Cyg A, which are not used in Methods A and B because they are beyond the cut-off frequency in many stellar models and therefore cannot be reliably determined in stellar models used for calibration, all of the frequencies listed in the table are used in the fits. Since the amplitude of the Helium signature is compared at a reference frequency rather than the average throughout the whole range covered in the fit, as is the case in Methods A and B, Method C is not anticipated to be sensitive to the presence of these modes in the observed frequency set. Furthermore, Method B, which requires the computation of second order differences, is unable to employ the two isolated l = 3 modes.

The fit to the glitch signatures using Method A is displayed in the upper panels of Figure-1. The distribution histograms of τHe and τCZ, which were produced by fitting 1000 re-alizations of data perturbed by adding random errors, are displayed in the lower panels. For both stars in the lower panels, it can be observed that the distribution of the fitted values of τCZ is incredibly wide with several peaks, even though the signature from the Helium ionization zone is robust and all data realizations produce values of τHe in a respectable range. For both 16 Cyg A & B, we find that the oscillatory signature from the convection zone base is weak. The CZ signature is hard to fit for some of the realizations. One of the secondary peaks in the τCZ distribution, according to an examination of the peaks, corresponds to τ = T0 − τCZ, where T0 is the star's acoustic radius. Aliasing may be the cause of this. We eliminate any realizations for which the main peak of the τCZ distribution does not contain the fitted value of τCZ. The estimate for τCZ is the median of the prominent peak. Only realizations with τCZ in the prominent peak are used to calculate additional fitted parameters.

Table 2: Observed oscillation frequencies for 16 Cyg A and B.

n	16 Cyg A				16 Cyg B			
	$l=0$ (μHz)	$l=1$ (μHz)	$l=2$ (μHz)	$l=3$ (μHz)	$l=0$ (μHz)	$l=1$ (μHz)	$l=2$ (μHz)	$l=3$ (μHz)
11	...	1334.39±0.03	1384.37±0.04	...	...	...	...	...
12	1391.64±0.04	1437.52±0.04	1488.35±0.10	...	...	...	1686.33±0.06	...
13	1495.00±0.06	1541.91±0.05	1591.24±0.11	...	1695.07±0.06	1749.18±0.05	1804.20±0.23	...
14	1598.69±0.07	1645.06±0.09	1694.19±0.17	...	1812.42±0.09	1866.52±0.10	1921.18±0.17	...
15	1700.91±0.08	1747.15±0.08	1795.76±0.10	1838.28±0.35	1928.90±0.07	1982.59±0.07	2036.68±0.12	2085.52±0.26
16	1802.32±0.07	1848.98±0.05	1898.28±0.10	1940.76±0.41	2044.27±0.06	2098.08±0.06	2152.40±0.10	...
17	1904.61±0.05	1952.00±0.05	2001.65±0.07	2045.92±0.23	2159.58±0.06	2214.16±0.06	2268.97±0.08	2319.21±0.22
18	2007.57±0.04	2055.53±0.05	2105.31±0.05	2149.91±0.14	2275.95±0.04	2331.14±0.04	2386.27±0.06	2436.79±0.18
19	2110.91±0.04	2159.15±0.04	2208.91±0.07	2253.54±0.17	2392.72±0.04	2448.25±0.04	2503.57±0.06	2554.15±0.15
20	2214.23±0.05	2262.54±0.05	2312.54±0.09	2357.37±0.18	2509.67±0.04	2565.40±0.04	2620.57±0.06	2671.75±0.15
21	2317.33±0.06	2366.26±0.06	2416.30±0.14	2462.08±0.37	2626.40±0.04	2682.41±0.05	2737.74±0.08	2789.19±0.27
22	2420.93±0.09	2470.32±0.08	2520.69±0.27	...	2743.33±0.06	2799.73±0.06	2855.68±0.14	2906.91±0.37
23	2525.14±0.20	2574.64±0.14	2624.15±0.37	2669.38±0.87	2860.77±0.11	2917.80±0.10	2973.47±0.25	3024.94±0.94
24	2629.21±0.21	2679.95±0.19	2727.41±1.64	...	2978.48±0.16	3036.08±0.16	3093.20±0.52	3144.36±0.68
25	2733.20±0.47	2784.18±0.37	...	...	3097.57±0.49	3154.42±0.27	...	...
26	2837.44±0.68	2891.30±0.84	...	...	3214.35±0.56	3272.94±0.74	...	...
27	2944.59±1.23	2996.53±1.02	...	...	...	...	...	...

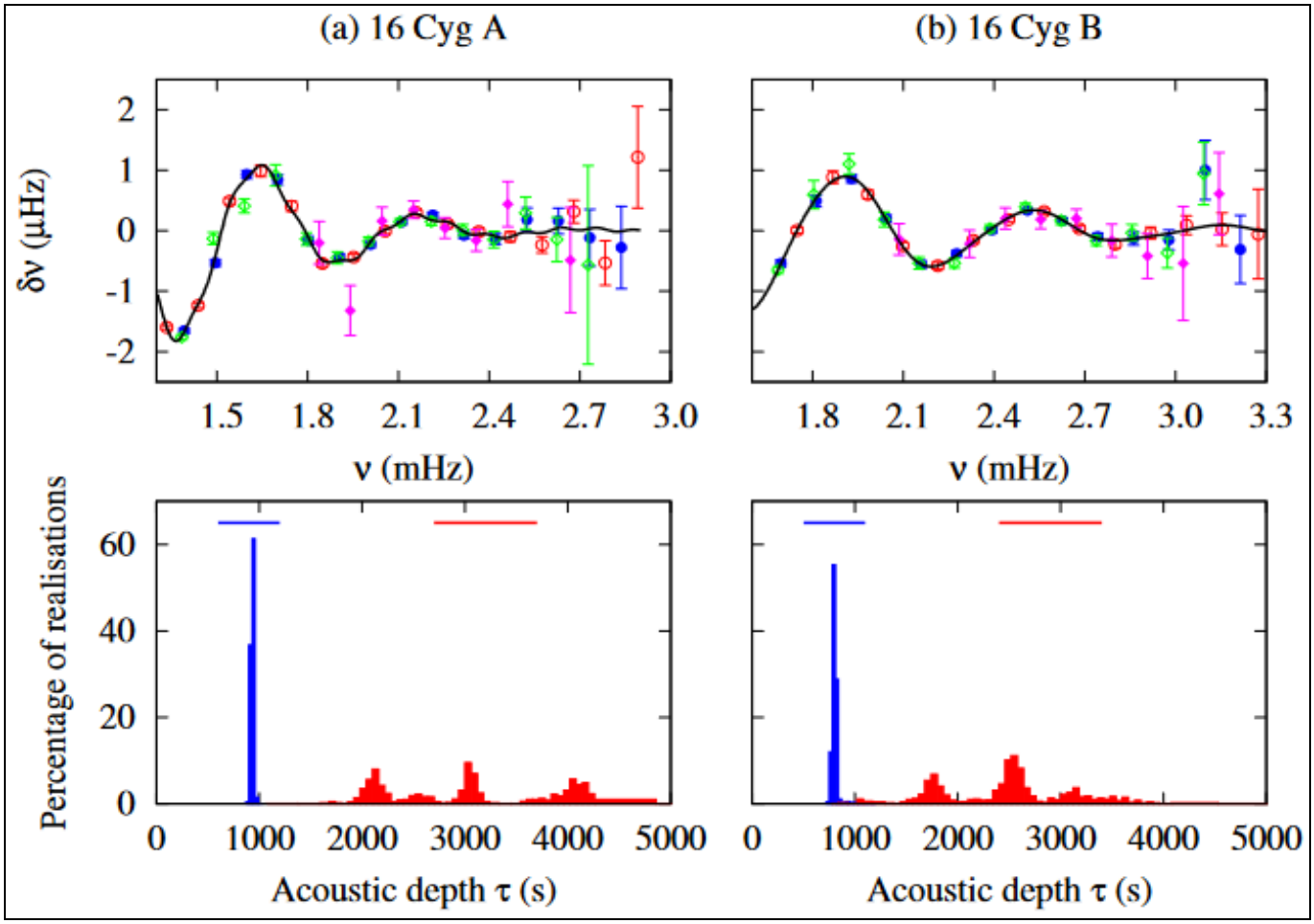

Fig 1: Fit to the observed frequencies of 16 Cyg A & B using Method A.

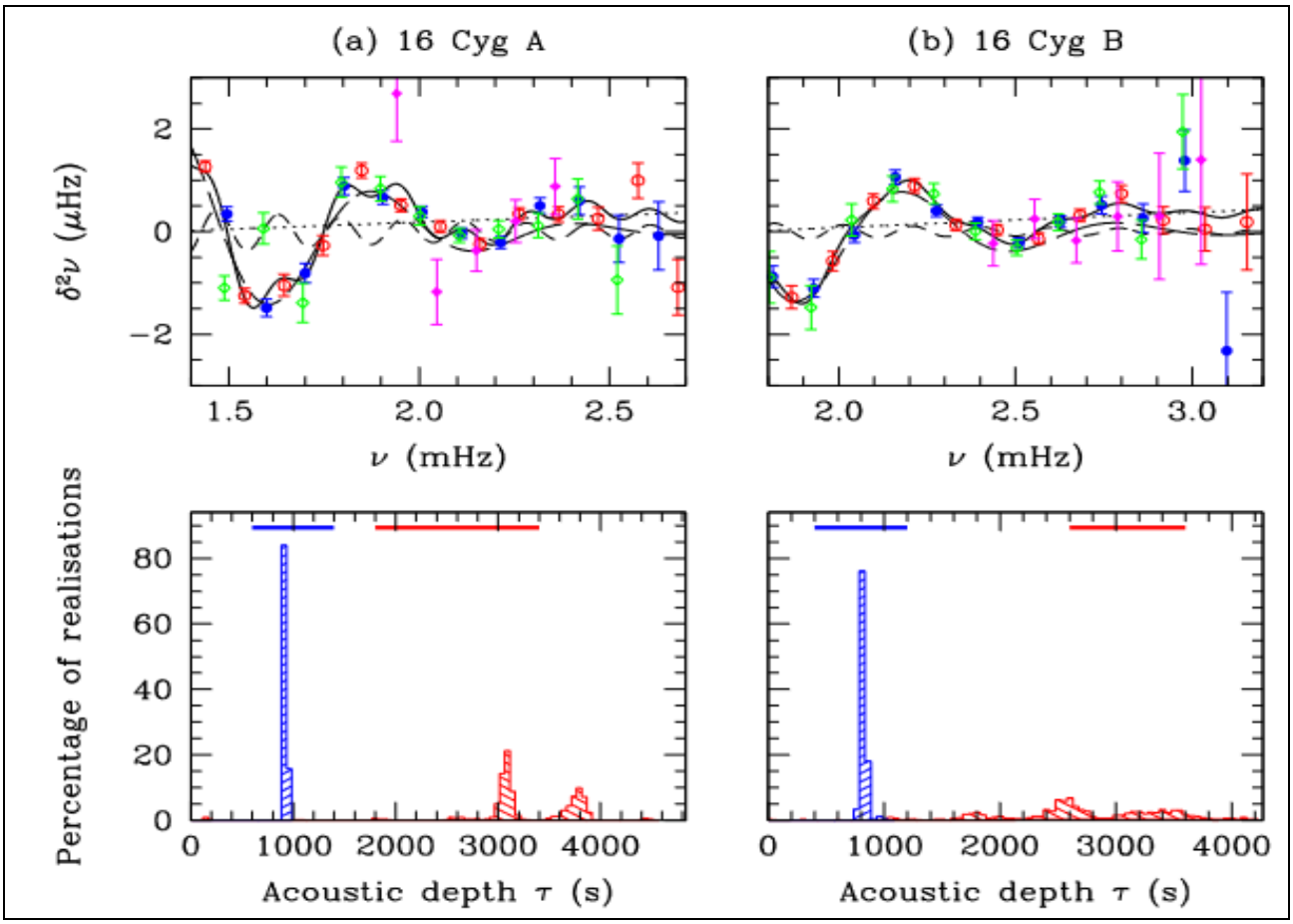

Fig 2: Fit to the second differences of 16 Cyg A & B using Method B.

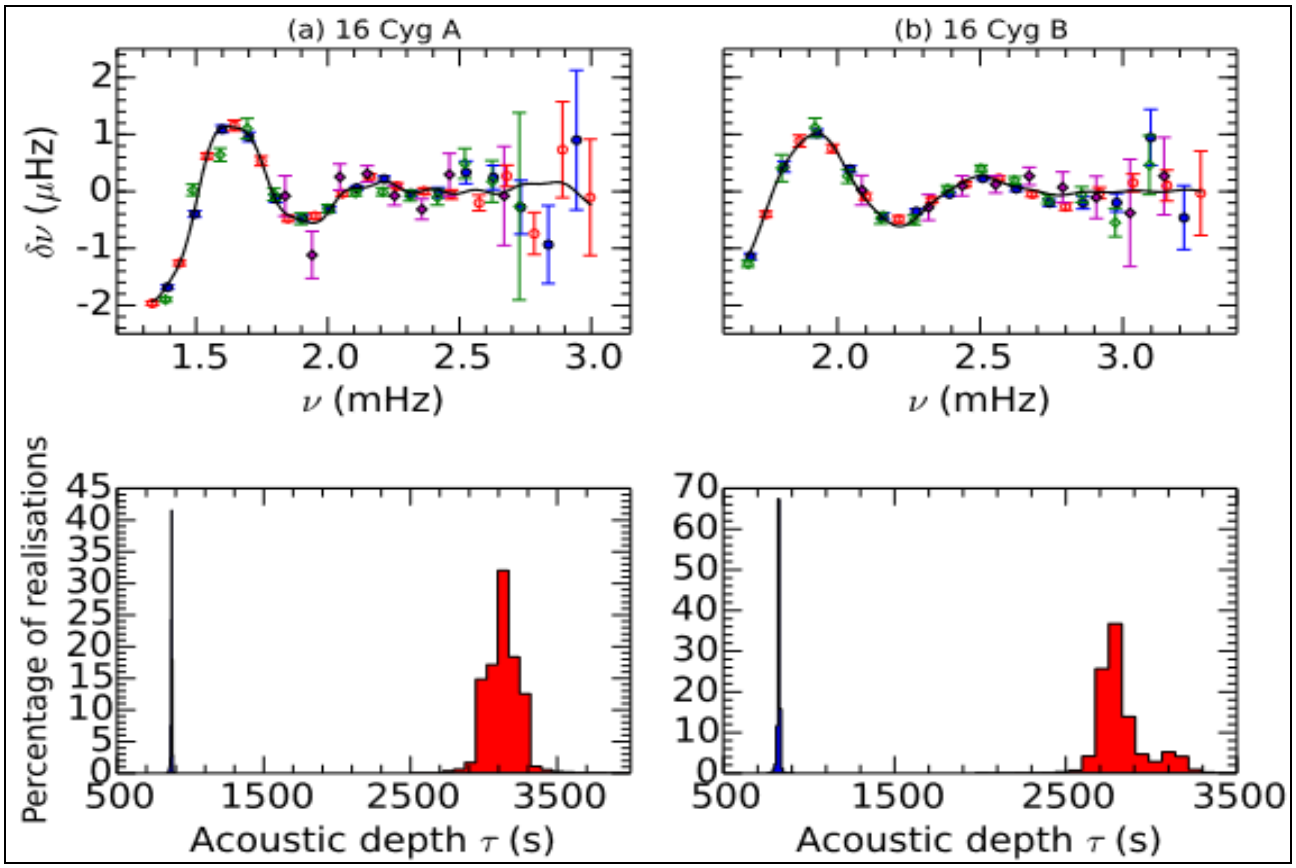

Fig 3: Fit to the observed frequencies of 16 Cyg A & B using Method C.

Table 3: Physical parameters obtained by fitting the observed frequencies of 16 Cyg A and B

Method	Amplitude of CZ Signal (μHz)	τ_{CZ} (s)	Amplitude of He Signal (μHz)	τ_{He} (s)
		16 Cyg A		
A	0.055 ± 0.012	3049 ± 57	0.508 ± 0.017	930 ± 14
B	0.072 ± 0.011	3079 ± 54	0.492 ± 0.013	919 ± 9
C	0.030 ± 0.012	3124 ± 110	0.435 ± 0.036	872 ± 4
		16 Cyg B		
A	0.044 ± 0.012	2536 ± 106	0.449 ± 0.018	801 ± 19
B	0.043 ± 0.010	2552 ± 147	0.421 ± 0.017	820 ± 17
C	0.048 ± 0.018	2775 ± 141	0.900 ± 0.031	824 ± 8

It should be noted that this chapter focuses on figuring out these stars' helium abundance rather than the location of the convection-zone base. Therefore, we fix the value of τCZ at several values around the main peak to examine whether our inability to fit τCZ reliably affects the Helium results. The fact that the fit to the He signature remains unchanged demonstrates how reliable the findings are with regard to Helium.

Table 3 shows the fitted values of the several physical parameters related to the He and CZ glitch. Note that the amplitude is computed at a reference frequency for Method C, whereas it is averaged throughout the fitting interval for Methods A and B. When the amplitudes of the second differences in Method B are converted back to the frequencies, the table shows that the oscillatory signatures derived using techniques A and B have equal amplitudes. This proves that the conversion factor is valid. The results are not affected by different types of oscillatory terms or by different strategies for eliminating the smooth component in the frequencies as a function of n, as seen by the close proximity of the fitted parameters using all three approaches.

Envelope Helium abundances of 16 Cyg A & B

Using the same modes and weights as the observations, the frequencies for the models are fitted in the same way. The amplitude of the He signature for each MESA model that was derived using Method A. The observed amplitude is also displayed in the figure. As you can see from the figure, the amplitude primarily depends on the models' present helium abundance. Variations in mass, effective temperature, and luminosity are the main causes of the scatter caused by other model parameters. Table-4 lists the helium abundances for both stars that were determined by calibrating the model amplitude with observation. MESA and YREC yielded He-lium abundances that are within error of one another. The helium abundances of 16 Cyg A and 16 Cyg B differ, albeit only by a little margin. All three approaches produce findings for 16 Cyg A that fall within error bars of one another, however for 16 Cyg B, Method A typically produces results that are greater than those of Method B. The two approaches differ by as much as 2.5σ. Systematic errors can be quantified by comparing the results of different approaches.

The modes at the low end of the spectrum are crucial to the accuracy of determining the abundance of helium. The accuracy of the estimate of helium abundance is greatly increased by the inclusion of a few low order modes or by any appreciable improvement in the precision of these modes. We repeat the fit using Method A to comprehend this improvement after increasing the uncertainty in the lowest three modes of degrees 0, 1, and 2 or after progressively eliminating the lowest order modes. We discover that in every instance, the uncertainty in the amplitude of the Helium signal soon increases by a factor of two or more. This could be because the signature's amplitude rapidly drops with frequency, and the low order modes help to stabilize the fit because the helium signature's amplitude is higher there. Consequently, a precise set of low order modes would be especially necessary to determine the helium content of a star.

Table 4: Helium abundances of 16 Cyg A and B.

Method	MESA		YREC
	GS98	AGSS09	GS98
	16 Cyg A		
A	0.250 ± 0.009	0.251 ± 0.009	0.249 ± 0.009
B	0.238 ± 0.009	0.243 ± 0.009	0.231 ± 0.009
C	0.239 ± 0.021	0.242 ± 0.023	0.236 ± 0.016
	16 Cyg B		
A	0.251 ± 0.010	0.254 ± 0.010	0.255 ± 0.009
B	0.263 ± 0.012	0.266 ± 0.012	0.257 ± 0.009
C	0.218 ± 0.013	0.228 ± 0.011	0.219 ± 0.009

The location of the acoustic glitches can be inferred from the oscillatory signature in the recorded frequencies. The acoustic depths of the He ionization zone and the base of the convection zone. Two methods are used to estimate the acoustic depths for the models: fitting the model frequencies or fitting the second differences of the model frequencies, and estimating the acoustic depth from the model's known sound-speed profile. The acoustic depth of each layer will be impacted by the uncertainties in the stellar surface characterization, which also affects the first estimate based on the sound-speed profile. The picture illustrates how the two estimates for a model agree well for τCZ, indicating a sensible choice of stellar surface. The number derived from the sound-speed profile, however, is consistently greater than the value derived from fitting the frequencies or the

Conclusion

We calculate the present Helium abundance and the depth of the He ionization zone using the oscillatory signature in the oscillation frequencies of 16 Cyg A & B, which is induced by the abrupt change of Γ1 in the Helium ionization zones.

We show that the observed frequencies can be used to properly estimate the Helium abundance of these stars. The three approaches produce consistent results for 16 Cyg A within the errorbars, but for 16 Cyg B, the results vary, albeit only by 2.5σ in the worst situation. It is discovered that the helium abundance for 16 Cyg A and 16 Cyg B ranges from 0.231 to 0.251 and 0.218 to 0.266, respectively. For 16 Cyg A, the observed value of τHe is greater than that in all chosen models, however the fitted value of τHe derived from observed frequencies for 16 Cyg B matches that derived from fitting the model frequencies. The other observed quantities that have been used to limit the models or some systematic mistakes in the modelling may be the cause of this.

The random errors resulting from those in the observed frequencies are represented by the error bars that are reported in Table-4. Furthermore, there would be systematic inaccuracies because of the uncertainties in the utilized stellar models and the approximate form of the oscillatory term. The first contribution, which is already included in the numbers mentioned above, can be inferred from the variations in values obtained using the three procedures. The equation of state, which converts the helium abundance to Γ1, should be the primary source of the stellar-model uncertainty. We do not anticipate much uncertainty on that count in these stars, where the uncertainties in the frequencies are significantly larger than those for the Sun, because it is known from extensive tests for the Sun that the OPAL equation of state is close to that of the Sun.

Because the surface corrections are a smooth function of n and mostly contribute to the smooth portion of the frequency, which can be distinguished from the oscillatory part, this method of measuring helium abundance is not very sensitive to the presence of surface effect. This is especially true for both stars under consideration, because the recorded frequencies span a large range of n values. Since the oscillatory signature can also be approximated with a polynomial of somewhat high degree, it may be challenging to distinguish the Helium signature from the smooth part if the observed frequency range is small. For this reason, Method B limits the polynomial's degree to the lowest statistically significant number. Higher degree polynomials can be utilized to approximate the smooth section thanks to the regularization employed in Methods A and C.

The present abundance in the stars' outer envelope is used to estimate the helium mass fraction. Naturally, due to the gravitational settling of helium, this number is lower than the original helium abundance of both stars. Assuming that the models of the two stars accurately reflect the quantity of Helium depleted due to settling, we may calculate the initial Helium abundance from the current one. MESA models for 16 Cyg A reveal a depletion of 0.048 ± 0.004 with the GS98 mixture and 0.054 ± 0.006 with the AGSS09 mixture. For 16 Cyg B models, the helium depletion is lower (0.043 ± 0.006 for GS98 and 0.048 ± 0.007 for AGSS09 combination). Both stars should have had the same initial composition because it is thought that the two parts of the binary system evolved from the same gas cloud. If so, there should be a 0.005 increase in the current helium abundance in 16 Cyg B's envelope compared to 16 Cyg A's. This discrepancy is consistent with the values we find. This discrepancy results from the two stars' slight mass differences. In a similar vein, the variations in convection zone thickness between the GS98 and AGSS09 mixtures are the cause of their differences. The helium depletion is lower in GS98 models because of their deeper convection zone. Therefore, the 16 Cyg system's initial helium abundance ranges from 0.28 to 0.31. This is comparable to the values discovered and somewhat greater than the value found. It was found that the solar initial helium abundance was 0.278 ± 0.006. In light of the greater metallicity of these stars, the estimations of Yi for the 16 Cyg system are therefore in agreement with solar values.

To determine whether the observed frequencies could differentiate between the various combinations, two sets of MESA models built with various heavy-element mixtures are employed. As anticipated, there is a difference in the depth of the convection zone between the two sets of models, with models built with the AGSS09 having a shallower convection zone and, therefore, lower τCZ than models with the GS98 mixture. However, the values of Y, τHe, and τCZ are very similar for both sets of models. However, the range for each set of models overlaps significantly. To differentiate between the two sets of models, the uncertainty in the value of τCZ derived from observed frequencies for 16 Cyg B is too great. If systematic modelling errors can be eliminated, it might be possible to use the models to differentiate between the two sets of models and gain an independent grasp of the debate over the abundance of solar heavy elements. For 16 Cyg A, the error in τCZ from observed frequencies is comparatively small.

References

1. Demarque P, Woo JH, Kim YC, Yi SK. Y2 isochrones with an improved core overshoot treatment. The Astrophysical Journal Supplement Series. 2004;155(2):667.
2. Marigo P, Girardi L, Bressan A, Groenewegen MA, Silva L, Granato GL. Evolution of asymptotic giant branch stars-II. Optical to far-infrared isochrones with improved tp-agb models. Astronomy & Astrophysics. 2008;482(3):883-905.
3. Dotter A, Chaboyer B, Jevremović D, Kostov V, Baron E, Ferguson JW. The Dartmouth stellar evolution database. The Astrophysical Journal Supplement Series. 2008;178(1):89.
4. Basu S, Antia HM. Helium abundance in the solar envelope. Monthly Notices of the Royal Astronomical Society. 1995;276(4):1402-1408.
5. Ramírez JG, Ramírez BS. Analyzing and interpreting continuous data using JMP: A step-by-step guide. SAS Publishing; c2009.
6. Houdek G, Gough DO. On the seismic age and heavy-element abundance of the Sun. Monthly Notices of the Royal Astronomical Society. 2011;418(2):1217-1230.